Maximum entropy estimation of directional wave spectra from an array of wave probes

OKEY NWOGU

Hydraulics Laboratory, National Research Council, Ottawa, Canada

A procedure for estimating directional wave spectra from an array of wave probes based on the Maximum Entropy Method (MEM) is developed in the present paper. The MEM approach yields an angular spreading function at each frequency band consistent with the input cross-spectral density matrix. The method is evaluated using numerical simulations of directional sea states. The MEM is also used to analyze data obtained from the three-dimensional wave basin of the Hydraulics Laboratory, National Research Council of Canada. Finally, the MEM is compared with the Maximum Likelihood Method (MLM) and is shown to be a powerful tool for directional wave analysis.

Key Words: directional wave analysis, maximum entropy method.

1. INTRODUCTION

Ocean waves are multi-directional, and information about the directional distribution of wave energy is often required for the design of coastal and offshore structures. Of all the methods currently used to resolve directional sea states, the MEM has been shown to have the highest directional resolving power.[5] The MEM has however only been used to analyze data from a wave probe-current meter array or a pitch-roll buoy. In laboratory applications, however, current meters have a relatively high level of noise present in the signals, leading to a degradation in the resolution of the MEM (see Nwogu *et al.*[7]). Wave probes currently used in laboratory wave basins have relatively lower noise to signal ratios than current meters. They are also less expensive and easier to calibrate, making them more convenient for use in laboratories for estimating directional wave spectra. This leads to the present development of an MEM procedure for the analysis of directional wave fields using a wave probe array.

The MEM has it's origins in probability theory[4] and has also been succesfully used in spectral analysis.[2] The spectral analysis approach is, however, based on the definition of the change in entropy. The directional spreading function can be thought of as the probability distribution of wave energy over direction and the definition of entropy used in probability theory is thus more justifiable as the basis of the MEM for the analysis of directional waves. This differs from the definition of change in entropy used by Barnard[1] for the analysis of directional wave fields.

The use of the concept of a directional spreading function to characterize a wave field should only apply to a spatially homogenous wave field with no correlation of the wave components travelling in different directions. The single summation, random phase method of wave synthesis (e.g. Miles and Funke[6]) produces such a wave field and is used in the present paper to simulate the water surface elevation time series at different wave probe locations. The cross-spectral density matrix is obtained from a Fast Fourier Transform (FFT) of the synthesized time series. The MEM procedure then uses the cross-spectral density matrix to estimate a directional spreading function for each frequency band.

2. THE MAXIMUM ENTROPY SOLUTION

For a spatially homogenous wave field, the cross-spectral density of the wave elevation at two locations x_m and x_n can be expressed as (see Isobe *et al.*[3])

$$S_{mn}(\omega) = S(\omega) \int_{-\pi}^{\pi} \exp\{ik \cdot (x_m - x_n)\} D(\omega, \theta)\, d\theta \tag{1}$$

where $D(\omega, \theta)$ is a nonnegative angular spreading function describing the distribution of wave energy over direction. The spreading function has to satisfy

$$\int_{-\pi}^{\pi} D(\omega, \theta)\, d\theta = 1 \tag{2}$$

The wave frequency, ω is related to the wavenumber, k by the linear dispersion relation. The directional wave spectrum can thus be defined as

$$S(\omega, \theta) = S(\omega) D(\omega, \theta) \tag{3}$$

where $S(\omega)$ is the conventional one-dimensional frequency spectrum. Equation (1) can be expressed as

$$\Phi_j(\omega) = \int_{-\pi}^{\pi} q_j(\theta) D(\omega, \theta)\, d\theta \quad j = 1, \ldots, M+1 \tag{4}$$

where $M = N(N-1)$, N is the number of wave probes

Accepted January 1989. Discussion closes March 1990.

$$q_j(\theta) = \begin{cases} \cos(kr_j \cos(\beta_j - \theta)) & j = 1, \ldots, M/2 \\ \sin(kr_j \cos(\beta_j - \theta)) & j = M/2 + 1, \ldots, M \\ 1 & j = M + 1 \end{cases} \quad (5)$$

$$\Phi_j(\omega) = \begin{cases} Re \dfrac{S_{mn}(\omega)}{[S_m(\omega)S_n(\omega)]^{1/2}} & j = 1, \ldots, M/2 \\ Im \dfrac{S_{mn}(\omega)}{[S_m(\omega)S_n(\omega)]^{1/2}} & j = M/2 + 1, \ldots, M \\ 1 & j = M + 1 \end{cases} \quad (6)$$

$$r_j = \sqrt{(x_m - x_n)^2 + (y_m - y_n)^2}$$

$$\beta_j = \tan^{-1}[(y_m - y_n)/(x_m - x_n)] \quad (7)$$

The entropy associated with the spreading function can be expressed as

$$E = -\int_{-\pi}^{\pi} D(\omega, \theta) \ln D(\omega, \theta)\, d\theta \quad (8)$$

Maximizing E subject to the constraints imposed by the cross-spectral density matrix (4) yields

$$D(\omega, \theta) = \exp\left\{-1 + \sum_{j=1}^{M+1} \nu_j q_j(\theta)\right\} \quad (9)$$

where ν_j Lagrange multipliers chosen to ensure the estimate of the spreading function is consistent with equation (4). Substitution of the maximum entropy solution (9) into equation (4) results in a nonlinear set of equations

$$\int_{-\pi}^{\pi} \exp\left\{-1 + \sum_{j=1}^{M+1} \nu_j q_j(\theta)\right\} q_i(\theta)\, d\theta = \Phi_i(\omega) \quad i = 1, \ldots, M+1 \quad (10)$$

The parameters ν_j cannot be easily determined analytically so one has to resort to an iterative technique. Most iterative procedures to determine the unknown Lagrange multipliers ν_j would have problems with convergence since some of the kernel functions $q_i(\theta)$ and $q_j(\theta)$ are correlated, depending on the relative spacing of the wave probes. The problem would have to be reformulated in terms of an orthogonal set of kernel functions.

Accordintg to well known theorems of linear algebra, a set of orthogonal functions $g_i(\theta)$ can be formed from $q_i(\theta)$ as

$$g = T^T q \quad (11)$$

where T is an orthogonal matrix with column vectors equal to the orthonormal eigenvectors of the covariance matrix defined by

$$Q_{ij} = \int_{-\pi}^{\pi} q_i(\theta) q_j(\theta)\, d\theta \quad (12)$$

The components of the covariance matrix can be

$$Q_{ij} \begin{cases} \pi[J_0(z_1) + J_0(z_2)] & i = 1, \ldots, M/2; \; j = 1, \ldots, M/2 \\ \pi[J_0(z_1) + J_0(z_2)] & i = M/2 + 1, \ldots, M; \; j = M/2 + 1, \ldots, M \\ 2\pi J_0(kr_i) & i = M + 1; \; j = 1, \ldots, M/2 \\ 2\pi J_0(kr_i) & i = 1, \ldots, M/2; \; j = M + 1 \\ 2\pi & i = M + 1; \; j = M + 1 \end{cases} \quad (13)$$

where

$$z_1 = k[(r_i \cos \beta_i - r_j \cos \beta_j)^2 + (r_i \sin \beta_i - r_j \sin \beta_j)^2]^{1/2}$$

$$z_2 = k[(r_i \cos \beta_i + r_j \cos \beta_j)^2 + (r_i \sin \beta_i + r_j \sin \beta_j)^2]^{1/2}$$

and J_0 is the Bessel function of the first kind of order zero. All other components of the covariance matrix are identically zero.

The existence of a zero eigenvalue of the matrix Q indicates that one of the functions $q_i(\theta)$ is either identically zero, or correlated with the other functions $q_j(\theta)$. Functions with zero eigenvalues are thus dropped and questions arise as to the relative importance of eigenvalues close to zero. If all the non-zero eigenvalues are retained, the solution procedure tends to become unstable. A criterion used to select a number of 'important' eigenvalues, L, is based on the ratio of each eigenvalue to the largest eigenvalue. In the present application, eigenvalues greater than 0.1% of the largest eigenvalue were considered to be important. The problem now is reduced to determining the parameters μ_j, $j = 1, \ldots, L$ which satisfy the nonlinear set of equations.

$$P_i = \int_{-\pi}^{\pi} g_i(\theta) \exp\left\{-1 + \sum_{j=1}^{L} \mu_j g_j(\theta)\right\} d\theta \quad i = 1, \ldots, L \quad (14)$$

where

$$P = T^T \Phi \quad (15)$$

The Levenberg–Marquardt algorithm is used to solve the system on non-linear equations for the parameters μ_j and the directional spreading function is now given by

$$D(\omega, \theta) = \exp\left\{-1 + \sum_{j=1}^{L} \mu_j g_j(\theta)\right\} \quad (16)$$

A suitable initial guess for the parameters μ_j can be determined from the linear approximation of the exponential function as

$$\exp\left\{-1 + \sum_{j=1}^{L} \mu_j g_j(\theta)\right\} \simeq \sum_{j=1}^{L} \mu_j g_j(\theta) \quad (17)$$

leading to initial guesses

$$\mu_j = P_j \quad j = 1, \ldots, L \quad (18)$$

The convergence criteria used to stop the iterative procedure requires that either the updated values of the μ's agree with the current values of the μ's to a specified accuracy, or that differences between the left and right hand sides of equation (14) be less than a specified tolerance. Due to the presence of noise and truncation of information provided by the original data set, the

above two criteria cannot be met in some cases and the solution is determined as that which minimized the square error in the iterative procedure. The square error E_Q is given by

$$E_Q = \left[\sum_{i=1}^{L}\left[P_i - \int_{-\pi}^{\pi} g_i(\theta)\exp\left\{-1 + \sum_{j=1}^{L}\mu_j g_j(\theta)\right\}\mathrm{d}\theta\right]^2\right] \tag{19}$$

The eigenvalue analysis is also useful for investigating different array spacings and configurations since it indicates the amount of redundant information in the available data. As an example, if a five probe array and a ten probe array have the same number of important eigenvalues, the additional information provided by the additional five probes can be considered to be redundant.

3. ANALYSIS OF SIMULATED AND MEASURED DATA

3.1 Numerically simulated data

The time series of the water surface elevation at different wave probe locations were synthesized using the single summation model described in Miles and Funke.[6] The water surface elevation is given by

$$\eta(x, y, t) = \sum_{i=1}^{N} A_i \cos[\omega_i t - k_i(x\cos\theta_i + y\sin\theta_i) + \varepsilon_i] \tag{20}$$

where A_i and ε_i are the amplitudes and phases of the wave components given by the random phase method as

$$A_i = \sqrt{2S(\omega_i)D(\omega_i, \theta_i)\,\Delta\omega\,\Delta\theta} \tag{21}$$
$$\varepsilon_i = 2\pi U[0, 1]$$

where $\omega_i = i(\Delta\omega/J)$ and $U[0, 1]$ is a uniform distribution from zero to one. The angles θ_i are chosen by a procedure such that the spreading function is approximated by J wave angles in each frequency band of width $\Delta\omega$. The angles can either be chosen randomly for each frequency component or chosen to vary linearly with frequency. The wave field produced by the single direction per frequency model is spatially homogenous and is thus more appropriate to use for checking directional wave analysis programs than the double summation model.

The first example considered is a JONSWAP incident wave spectrum with $f_p = 0.4$ Hz and $\gamma = 3.3$. The angular spreading is given by the frequency independent cosine spreading function

$$D(\theta) = \frac{1}{\sqrt{\pi}}\frac{\Gamma(s+1)}{\Gamma(s+\frac{1}{2})}\cos^{2s}(\theta) \qquad |\theta| < \pi/2$$
$$= 0 \qquad \text{otherwise} \tag{22}$$

where Γ is the gamma function and the parameter s is a spreading index describing the degree of wave short-crestedness with $s \to \infty$ representing a long-crested wave field. The array used for the directional wave analysis consists of five wave probes arranged in the layout shown in Fig. 1. The configuration is similar to the

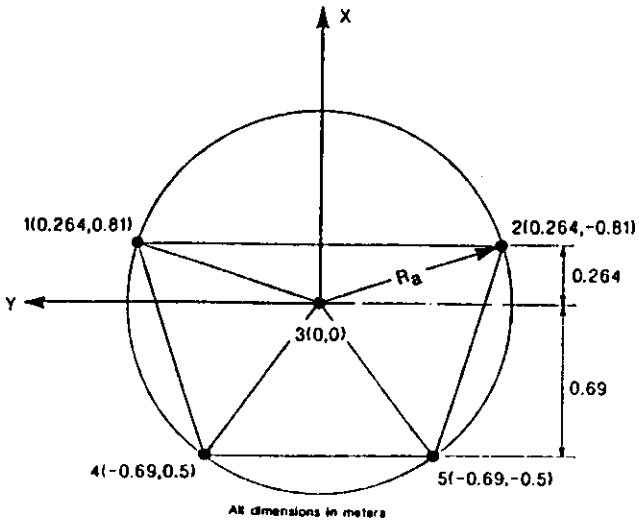

Figure 1. Arrangement of five probe array

CERC array used by Panicker and Borgman.[8] The water surface elevation time series at the different probe locations were synthesized for a duration of 819.2 s using a frequency bandwidth of 0.02 Hz and 32 wave directions per frequency band.

The FFT analysis was performed using the same bandwith used in the synthesis. Figure 2 shows a comparison of the target JONSWAP spectrum with the synthesized wave spectrum for the central probe. As expected, the synthesized spectrum matches the target spectrum fairly well. The slight differences are due to the wide frequency band used. Figures 3 to 5 show the target, MEM and MLM (see Isobe *et al.*[3]) estimated angular spreading functions at the peak frequency for $s = 1$, 5 and 20 respectively. The specified mean direction $\theta_0 = 0°$. It can be seen that the MEM estimates the specified spreading functions better than the MLM for all cases. The fit is however better for the higher spreading indices. The MLM always estimates a broader spreading function because it does not satisfy the constraints imposed on the cross-spectral density matrix of the original data (equation (1)).

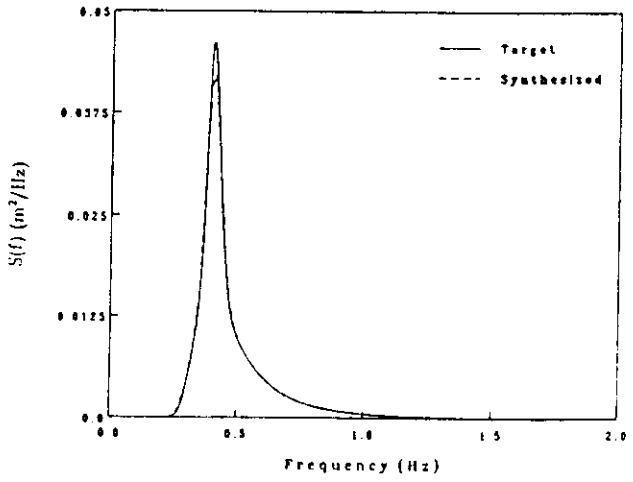

Figure 2. Comparison of target and synthesized JONSWAP spectra (fp = 0.4 Hz, γ = 3.3) at the central probe of the array

limited white noise from zero to the Nyquist frequency to the synthesized time series. Figure 6 shows a comparison of the target and MEM estimated spreading functions at the peak frequency for $s = 5$ with 0% and

not seem to affect the resolution of the MEM at the peak frequency appreciable. Figures 7 and 8 show plots of the mean direction and standard deviation of the wave propagation angle relative to the estimated mean direction over the frequency range $0.65f_p$ to $2f_p$. Both

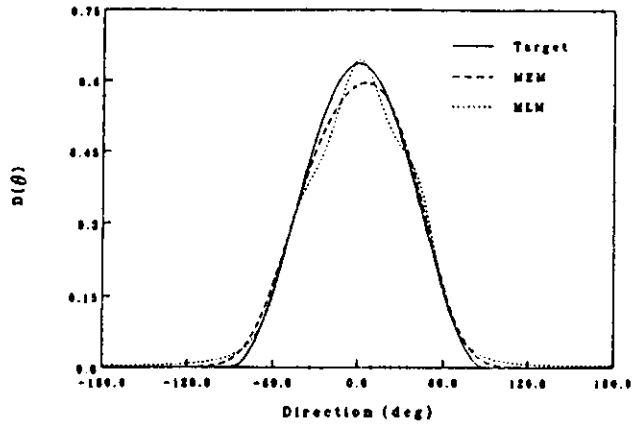

Figure 3. Comparison of target, MEM, and MLM directional spreading functions (s = 1, f = fp)

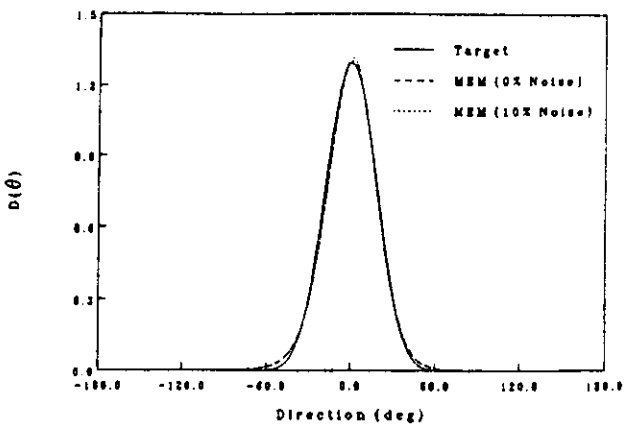

Figure 6. Comparison of target and MEM directional spreading functions with noise (s = 5, f = fp)

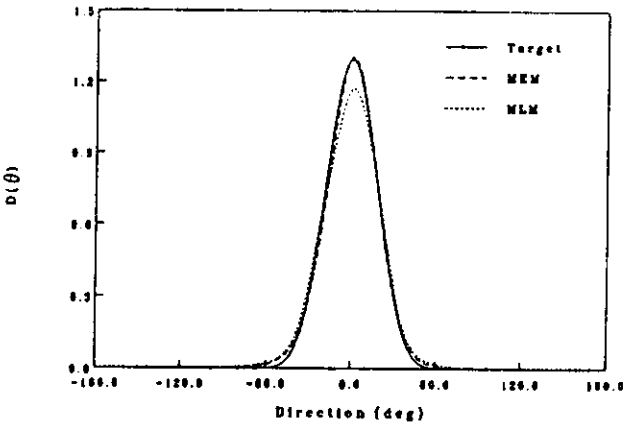

Figure 4. Comparison of target, MEM, and MLM directional spreading functions (s = 5, f = fp)

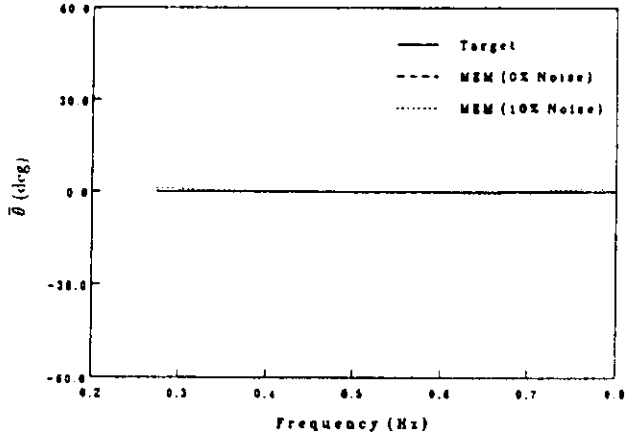

Figure 7. Comparison of target and MEM estimated mean direction of wave progagation (s = 5)

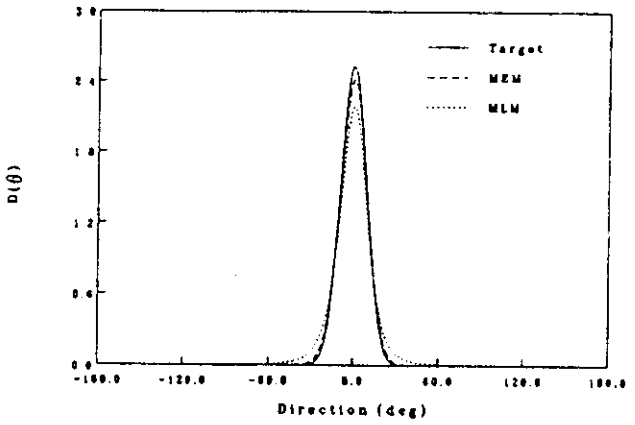

Figure 5. Comparison of target, MEM, and MLM directional spreading functions (s = 20, f = fp)

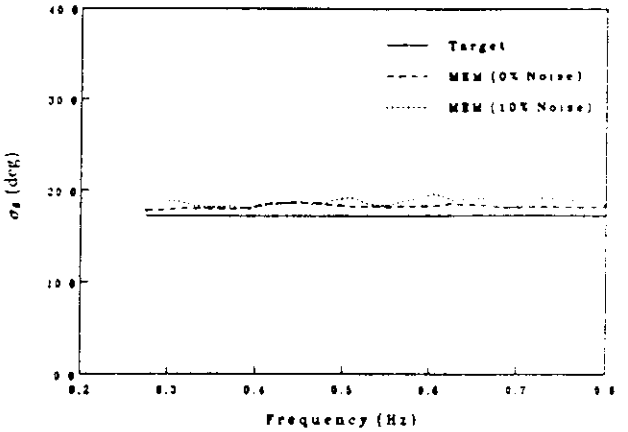

Figure 8. Comparison of the standard deviations of the directional spreading functions (s = 5)

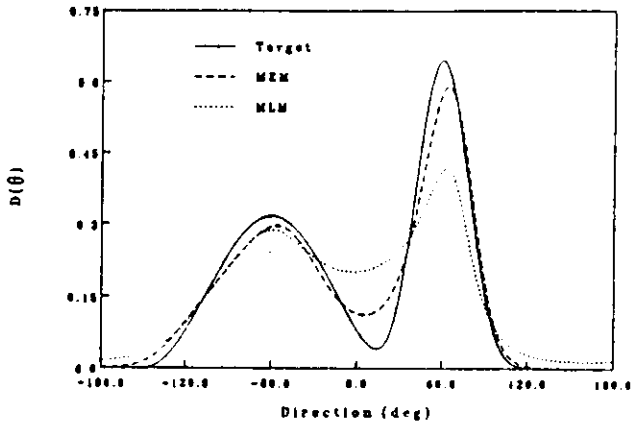

Figure 9. Comparison of target, MEM, and MLM spreading functions for a bidirectional sea state ($f = fp$)

quantities are not noticeably affected by the 10% noise in the specified frequency range.

A bidirectional sea state with the same JONSWAP spectrum as the previous example was simulated by interlacing the frequencies of the two principal wave trains so as to produce a spatially homogenous wave field. One wave train had a principal direction $\theta_0 = 60°$ and a spreading index $s = 5$ while the other wave train had $\theta_0 = -60°$ and $s = 1$. Figure 9 shows a comparison of the target, MEM and MLM estimated spreading functions at the peak frequency. The MEM resolves such a bidirectional sea state much better than the MLM.

3.2 Laboratory data

Tests were carried out in the multidirectional wave basin of the Hydraulics Laboratory, National Research Council of Canada. The basin is 30 m × 19.2 m and 3 m deep. Tests were carried out in a water depth of 2 m. The basin is equipped with a 60 segment, multi-mode wave generator capable of producing regular and random long- and short-crested sea states. Figure 10 shows a side view of the wave generator. Energy absorption beaches are located along the other three sides of the basin.

A wave probe array was used to obtain information about wave directionality in the basin. The wave gauge array consisted of nine capacitance type wave probes mounted on a rigid frame attached to vertical posts as shown in Fig. 11. All nine wave probes can be calibrated at the same time by remotely moving the frame containing the probes vertically along the posts in still water. The spacing of the outer five probes is the same as that used for the numerical simulations (Fig. 1). The inner five probes have the same configuration but are at a half the radius of the enclosing circle.

Tests were carried out for a JONSWAP incident wave spectrum with significant wave height, $Hmo = 0.22$ m, $fp = 0.5$ Hz and different specified cosine power angular spreading functions. Data was collected at a sampling frequency of 10 Hz for 819.2 s which was the recycling period used for the generation of the waves. The FFT cross-spectral density estimates were smoothed over frequency bands of width $\Delta f = 0.04$ Hz.

Figure 12 shows a comparison of the specified and measured frequency spectrum for the central wave probe. The spectrum of the measured water surface elevation matches the specified spectrum rather well. Figures 13 and 14 show a comparison of the MEM estimated spreading functions using the outer five probes and all nine probes for target spreading indices $s = 3$ and 6 respectively. It can be seen that there is very little difference between the spreading functions estimated using the five probe array and the nine probe array. The information provided by the additional four probes can thus be considered to be redundant. There is a slight

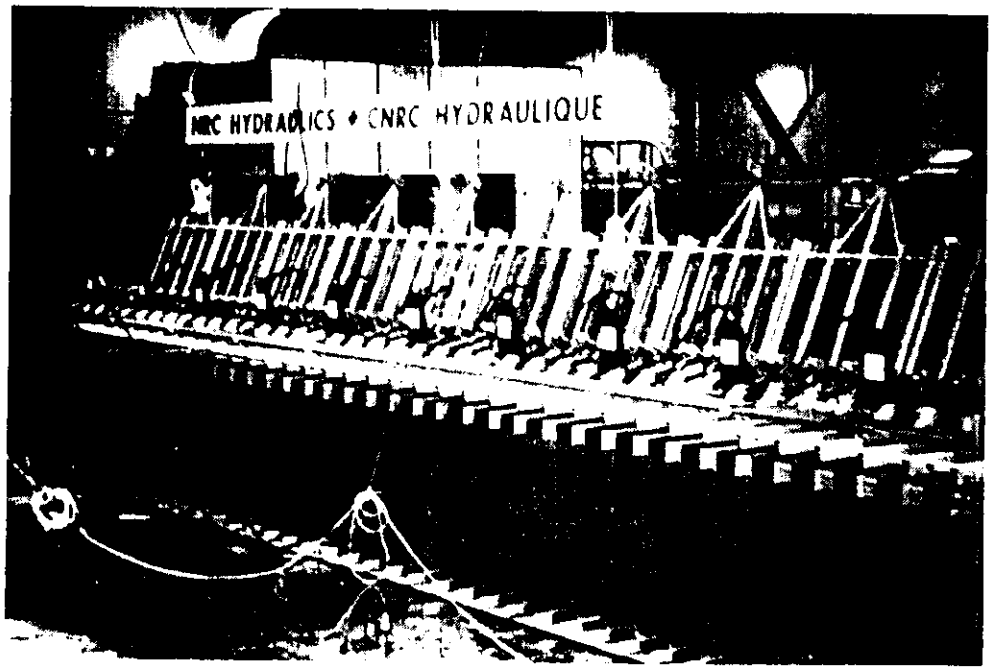

Figure 10. View of Segmented Wave Generator

probably due to the fact that no attempt was made to align the probe array carefully with respect to the x axis of the Basin.

In general, it was observed that the CERC five probe array is adequate for the resolution of directional sea states by the MEM. It was however thought useful to

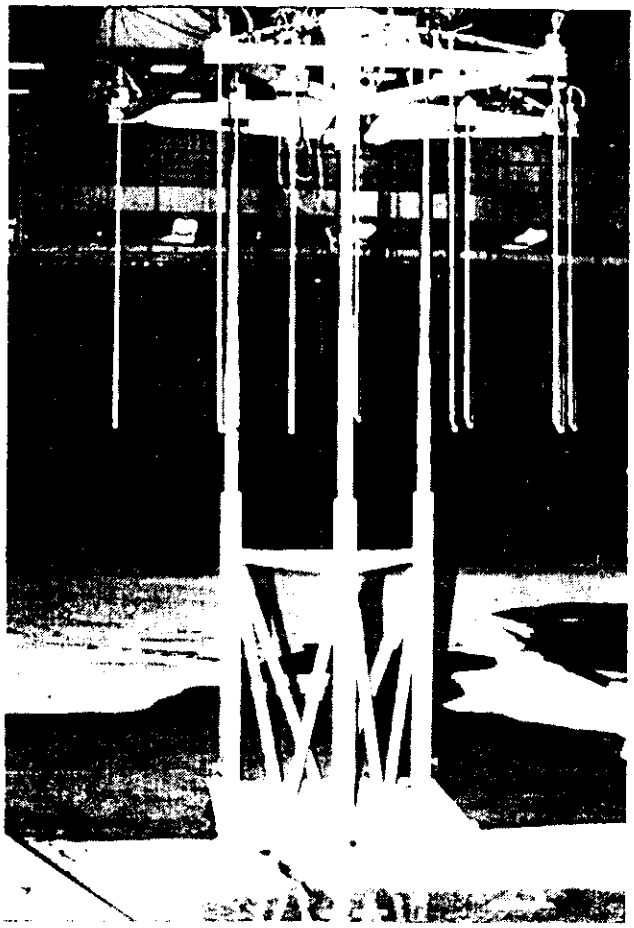

Figure 11. View of nine probe array

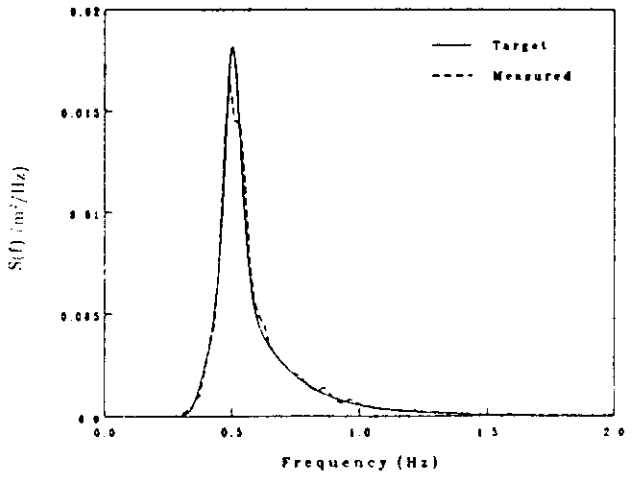

Figure 12. Comparison of target and measured JONSWAP spectra (fp = 0.5Hz, Hs = 0.22 m) at the central probe of the array

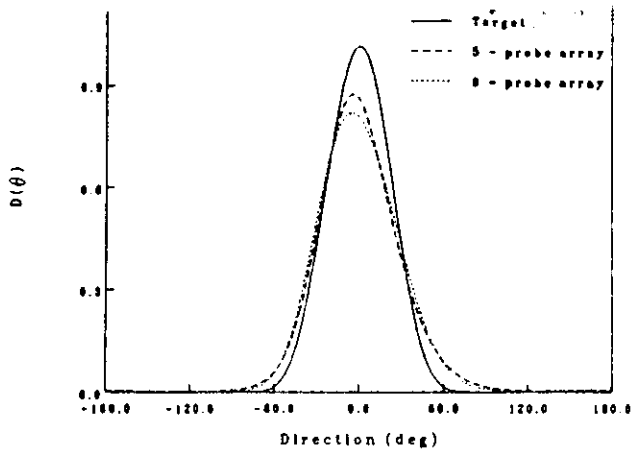

Figure 13. Comparison of target and measured directional spreading functions for a five and nine probe array (s = 3, f = fp)

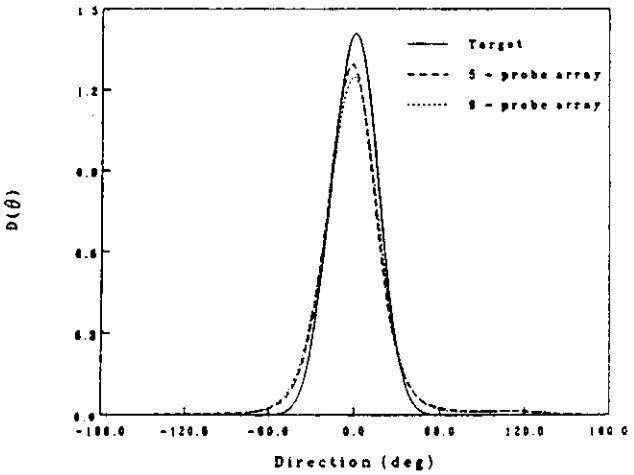

Figure 14. Comparison of target and measured directional spreading functions for a five and nine probe array (s = 6, f = fp)

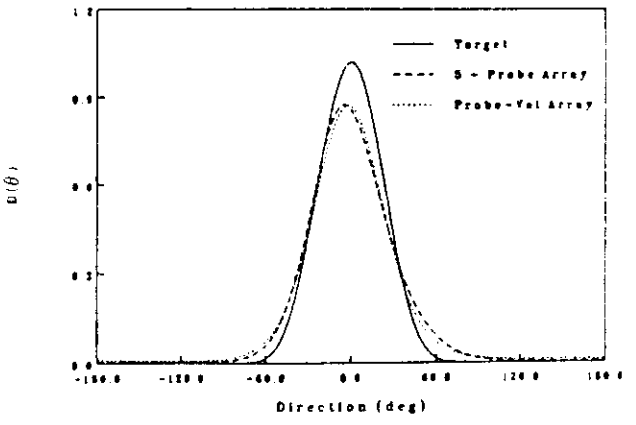

Figure 15. Comparison of target and measured directional spreading functions for a five probe and probe-current meter array (s = 3, f = fp)

determine for what range of wavelengths should either the outer five probes or inner five probes be used. The arrays provide an adequate resolution of directional wave spectra when the ratio of the array radius, R_a to the wavelength, L is in the range of 0.05 to 0.5 with optimum resolution at a ratio of about 0.15.

The results from a wave probe array were also compared with that from a wave probe – current meter array. Figure 15 shows a comparison of the estimated spreading functions using the two arrays for $s = 3$ at the peak frequency. In the absence of measurement noise, there is very little difference between the spreading functions estimated using the probe array and probe – current meter array in a spatially homogenous wave field.

CONCLUSIONS

A method for estimating directional wave spectra from a wave gauge array using the maximum entropy principle has successfully been developed. The MEM yields a spreading function of each frequency band which is consistent with the cross-spectra of the measured water surface elevation time series.

The MEM was compared with the MLM for different directional sea states and was shown to resolve directional seas consistently better than the MLM, particularly for bidirectional seas. The tests also indicate that the CERC five probe array is adequate for the resolution of most directional sea states.

Due to the truncation of redundandant information from the original data set in the eigenvalue analysis and the presence of noise, the MEM solution might in some cases not exactly satisfy the constraints imposed by the cross-spectral density matrix, but would minimize the introduced error in a least square sense.

ACKNOWLEDGEMENTS

This work was completed while the author was a guest worker at the Hydraulics Laboratory, National Research Council of Canada and was partially supported by NRCC Contract No. 043-1397/7207. The assistance provided by Messrs E. R. Funke, M. D. Miles and Dr. E. P. D Mansard is gratefully acknowledged.

REFERENCES

1 Barnard, T. E. Analytical studies of techniques for the computation of high-resolution wavenumber spectra, Texas Instruments Advanced Array Research, Spec. Rep. No. 9, 1969
2 Burg, J. P. Maximum entropy spectral analysis, Proc, 37th Annual Int. Soc. Explor. Geophys. Meeting, Oklahoma City 1967
3 Isobe, M., Kondo, K. and Horikawa, K. Extension of MLM for estimating directional wave spectrum, Proc, Symp. on Description and Modelling of Directional Seas, Copenhagen, 1984
4 Jaynes, E. T. Information theory and statistical mechanics, Papers I and II, *Phys. Rev.* 1957, **106**, 108
5 Kobune, K. and Hashimoto, N. Estimation of directional spectra from the maximum entropy principle, Proc. 5th Int. Offshore Mechanics and Arctic Engineering Symp., Tokyo, Japan, Vol. I. 80–85
6 Miles, M. D. and Funke, E. R. A comparison of methods for synthesis of directional seas, Proc. 6th Int. Offshore Mechanics and Arctic Engineering Symp., Houston, 1987, Vol. II, 247–255
7 Nwogu, O. U., Mansard, E. P. D., Miles, M. D. and Isaacson, M. Estimation of directional wave spectra by the maximum entropy method, Proc. IAHR Seminar on Wave Generation and Analysis in Laboratory Wave Basins, Lausanne, Switzerland
8 Panicker, N. N. and Borgman, L. E. Directional spectra from wave gauge arrays, Hydrogr. Eng. Lab. Rep. HEL-16, University of California, Berkely, 1970